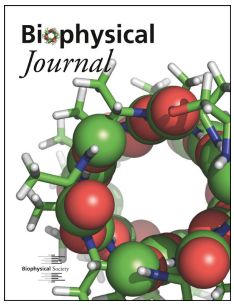

Functional analysis of Ctenophore Shaker K^+ channels: N-type inactivation in the animal roots

Benjamin T. Simonson, Max Jegla, Joseph F. Ryan, Timothy Jegla

PII: S0006-3495(24)00068-7

DOI: https://doi.org/10.1016/j.bpj.2024.01.027

Reference: BPJ 12940

To appear in: *Biophysical Journal*

Received Date: 26 September 2023

Accepted Date: 24 January 2024

Please cite this article as: Simonson BT, Jegla M, Ryan JF, Jegla T, Functional analysis of Ctenophore Shaker K^+ channels: N-type inactivation in the animal roots, *Biophysical Journal* (2024), doi: https://doi.org/10.1016/j.bpj.2024.01.027.

Title: *Functional analysis of Ctenophore Shaker K⁺ channels: N-type inactivation in the animal roots*

Running Title: *Origins of N-type inactivation in Shaker*

Authors and Affiliations: Benjamin T. Simonson[1], Max Jegla[1], Joseph F. Ryan[2,3] and Timothy Jegla[1*]

[1]Department of Biology and Huck Institutes of the Life Sciences, Penn State University, University Park, PA

[2]Whitney Laboratory for Marine Bioscience, University of Florida, St. Augustine, FL

[3]Department of Biology, University of Florida, Gainesville, FL

[*]Correspondence: Timothy Jegla, Department of Biology, Penn State University, University Park, PA, 814-865-1668, tjj3@psu.edu.

ABSTRACT

Here we explore the evolutionary origins of fast N-type ball and chain inactivation in Shaker (Kv1) K^+ channels by functionally characterizing Shaker channels from the ctenophore (comb jelly) *Mnemiopsis leidyi*. Ctenophores are the sister lineage to the rest of animals and *Mnemiopsis* has > 40 Shaker-like K^+ channels, but they have not been functionally characterized. We identified three *Mnemiopsis* channels (MlShak3-5) with N-type inactivation ball-like sequences at their N-termini and functionally expressed them in *Xenopus* oocytes. Two of the channels, MlShak4 and MlShak5 showed rapid inactivation similar to cnidarian and bilaterian Shakers with rapid N-type inactivation while MlShak3 inactivated ~100-fold more slowly. Fast inactivation in MlShak4 and MlShak5 required the putative N-terminal inactivation balls sequence. Furthermore, the rate of fast inactivation in these channels depended on the number of inactivation balls/channel, but the rate of recovery from inactivation did not. These findings closely match the mechanism of N-type inactivation first described for *Drosophila* Shaker in which 1) inactivation balls on the N-termini of each subunit can independently block the pore, and 2) only one inactivation ball occupies the pore binding site at a time. These findings suggest classical N-type activation evolved in Shaker channels at the very base of the animal phylogeny in a common ancestor of ctenophores, cnidarians and bilaterians and that fast-inactivating Shakers are therefore a fundamental type of animal K^+ channel. Interestingly, we find evidence from functional co-expression experiments and molecular dynamics that MlShak4 and MlShak5 do not co-assemble, suggesting that *Mnemiopsis* has at least two functionally independent N-type Shakers channels.

SIGNIFICANCE STATEMENT

Classic N-type ball and chain inactivation characterized by Aldrich and colleagues using the *Drosophila* Shaker K^+ channel represents a fundamental mechanism for fast inactivation in diverse voltage-gated ion channels. N-type inactivation is widespread in bilaterian and cnidarian Shaker channels, but the state of Shaker N-type inactivation in the last common ancestor of animals has remained a mystery. Here we express native ctenophore (comb jelly) Shaker channels for the first time to the best of our knowledge and identify classic N-type inactivation in two of them. Ctenophores are believed to be the earliest diverging animal lineage and Shaker K^+ channels first emerged in a common ancestor of ctenophores, cnidarians and bilaterians. This finding therefore suggests that fast inactivating N-type Shakers may have been part of the original animal ion channel tool kit.

INTRODUCTION

Hodgkin and Huxley planted the seed that inactivation in voltage-gated ion channels could be caused by a physical particle in their revolutionary 1952 description of the gating of Na^+ and K^+ conductances in the squid giant axon (1). In their model, inactivation of the Na^+ conductance was caused by a single physical gating particle that they proposed to move within the membrane. In the 1970s Armstrong and Bezanilla (2,3) showed that Na^+ channel inactivation was in actuality dependent on a cytoplasmic domain that could be removed by proteolytic cleavage, and they described Na^+ inactivation as a "ball and chain" mechanism in which a tethered cytoplasmic inactivation domain occluded the pore after channel activation. More recently, it has been proposed that Na^+ channel inactivation may involve closure of the inner pore akin to a new inactivation mechanism described for Kv2.1 and Kv4.2 potassium channels (4,5). Nevertheless, the idea of ball and chain inactivation drove early mechanistic studies and the first detailed molecular description of true ball and chain inactivation came over a decade after it was originally proposed for Na^+ channels when Hoshi, Aldrich and Zagotta dissected the mechanism of fast inactivation in the A/B splice variants of the cloned *Drosophila* voltage-gated K^+ channel Shaker (6,7). They called this rapid Shaker ball and chain inactivation N-type inactivation because the inactivation ball was formed by the N-terminus of the channel, distinguishing it from C-type inactivation that derives from conformational changes in the outer pore (8,9). Similar N-type ball and chain inactivation has since been described in diverse K^+ channels (recently reviewed in detail by Sukomon *et al*. (10)) and it thus represents a fundamental mechanism for rapid inactivation in voltage-gated channels. Our goal here is to celebrate Hoshi, Zagotta and Aldrich's groundbreaking work by exploring the evolutionary history of N-type inactivation in Shaker channels themselves. Where did those fast-inactivating Shaker channels come from, do they all use the same N-type inactivation mechanism, and what might animals need them for?

Drosophila Shaker was the first K^+ channel cloned (11-13) and the founding member of the animal family of voltage-gated K^+ channels that we will refer to here as the Shaker gene family. This gene family is comprised of the Shaker (Kv1), Shab (Kv2), Shaw (Kv3) and Shal (Kv4) gene subfamilies (14-17). Unless specified as "Shaker family", we will use the term Shaker to refer to the Shaker or Kv1 subfamily in this paper. Shaker family genes encode subunits that share a unique domain structure among K^+ channels consisting of a cytoplasmic T1 domain in the proximal N-terminus (18,19) coupled to a transmembrane channel core consisting of a 4 transmembrane domain voltage-sensor domain (VSD) and a two transmembrane domain pore domain (PD) (20). Channels function as tetramers with four domain-swapped VSDs at the periphery gating a single central K^+-selective pore (20,21). The T1s mediate subfamily specific assembly via formation of a tetrameric ring in the cytoplasm (19,20,22,23). Assembly restriction allows for multiple functionally distinct Shaker family potassium channels from different subfamilies to be expressed in a single neuron and thus increases signaling complexity. The tetrameric structure of these channels also has a direct impact on N-type inactivation in that channels can have up to four inactivation balls, one for each subunit (Fig. 1A). However, only a single ball occupies the conduction pathway in the inactivated state (Fig 1A). The rate of N-type inactivation is thus dependent on the number of subunits with inactivation balls, but the rate of recovery from inactivation is not (24).

Understanding the evolutionary history of the Shaker family as a whole and Shaker subfamily N-type inactivation in particular requires a quick introduction to the revised animal phylogeny in the era of whole genome comparisons (Fig. 1B). The three major groups of animals of interest for the evolution of Shaker family channels are Bilateria, Cnidaria and Ctenophora. Bilaterians include all the major animal model organisms and form a sister clade with Cnidarians (jellyfish, corals, anemones) with a divergence time roughly 600-700 million years ago based on molecular clocks (25-27). Together with placozoans, they form a clade of

animals coined Parahoxozoa based on their unique, shared homeodomain protein complement (28). Similar to most parahoxozoans, Ctenophores, or comb jellies, have nervous systems but surprisingly appear to have diverged at the base of the animal phylogeny before the branching points of placozoans and sponges (Fig. 1B). Ctenophores lack many characteristic neuronal gene families shared among cnidarians and bilaterians, sometimes because of loss, but often due to absences of those genes in the metazoan common ancestor (29-32). The Shaker, Shab, Shaw and Shal Kv subfamilies were shown to be conserved across Bilateria soon after their initial discovery in *Drosophila* (14,15), and all four are also conserved across Cnidaria (16,17,33-35). However, only the Shaker subfamily has been found in ctenophores, though it is highly expanded in the genome of *Mnemiopsis leidyi* (16). Thus, the Shaker subfamily is the most ancient extant subfamily of the broader Shaker gene family and can be traced to the very base of the animal phylogeny. It is surprisingly ctenophores and cnidarians that have the largest and most diverse sets of Shaker subfamily genes (16,17), so Shaker family channel diversification does not track with physiological and anatomical complexity on an organismal level.

But what about the evolution of the classic N-type inactivating Shaker first characterized in *Drosophila*? At first it appeared that it might not represent a conserved Shaker phenotype because none of the eight mammalian Shakers (Kv1.1-1.8) has similarly fast intrinsic N-type inactivation. However, it was later discovered that vertebrate Shakers can include a β-subunit that confers rapid inactivation with their own N-terminal ball (36,37). Fast inactivating Shakers have also been found in crustaceans (38), flatworms (39) and mollusks (40), suggesting that functional homologs of the Shaker A/B variants first characterized by Aldrich and colleagues are widespread among bilaterian invertebrates. One exception may be the nematode *C. elegans* where only slow inactivating Shaker currents have been genetically identified to date (41,42). Twelve Shaker subfamily channels are conserved across Cnidaria (17), and N-type inactivation is across the phylum in orthologs of the *Nematostella vectensis* channel NvShak1 (33,35,43). NvShak4 and NvShak5 also show classic N-type inactivation (35), but conservation of the phenotype in those channel ortholog groups has not been examined. The direct evolutionary relationships between bilaterian and cnidarian N-type inactivating Shakers are not clear due to independent molecular and functional diversification of the subfamily in the two phyla (16,17,35). N-type inactivation may be relatively easy to evolve *de novo* since it has evolved independently in vertebrate Kvβs, a subset of vertebrate Shaw (Kv3) channels (44) and cnidarian Shal (Kv4) channels (34). Interestingly, the vertebrate Kv3.4 ball inactivates Shaker channels (44-46), suggesting that the conduction pathway receptor sites might be quite similar across the Shaker family. This receptor promiscuity coupled with the relatively loose sequence requirements for N-terminal balls (10) would be expected to increase the evolutionary plasticity of N-type inactivation. Nevertheless, a large majority of cnidarians and bilaterians appear to have both rapidly inactivating N-type Shakers and Shakers with slow or no N-type inactivation (17,45) suggesting that both of these Shaker types were present in the last common ancestor of these two lineages and there has been strong evolutionary pressure to maintain both of these Shaker types.

But can the classic N-type inactivating Shaker be traced to the last common ancestor of all extant animals? If so, then fast inactivating N-type Shakers should also be found in ctenophores, those earliest diverging animals. Here we show that the ctenophore *Mnemiopsis leidyi* does indeed have at least two Shaker channels with rapid N-type inactivation. Thus, the classic fast inactivating *Drosophila* Shaker A/B variant that Aldrich and colleagues used to characterize N-type inactivation appears to be a functional ortholog of a fundamental channel type present in the original animal K^+ channel toolkit.

MATERIALS AND METHODS

Cloning and transcript Synthesis

Wild type (WT) expression constructs were synthesized (Twist Bioscience, San Francisco, CA) using *Xenopus* optimized codons and surrounded by *Xenopus* β-globin UTR sequences from the pOX expression vector (34). A T3 RNA polymerase promoter was included upstream for *in vitro* transcription and the whole construct was inserted the pET-21(+) expression vector at the EcoRI and NotI restriction sites. Full plasmids were sequence verified; DNA sequences and channel amino acid sequences are included in Table S1.

For plasmid expression vectors, capped transcripts for expression in *Xenopus* oocytes were synthesized *in vitro* using the T7 mMessage mMachine kit from Not I linearized plasmids, purified via LiCl precipitation and resuspended for injection in nuclease-free water. For N-terminal truncated or switched constructs, the expression cassette was amplified by PCR from WT plasmids with a sense primer containing the T3 promoter followed by a Kozak consensus sequence and the construct the engineered coding sequence and an antisense primer at the end of the 3' UTR. PCR products were verified by gel electrophoresis, column purified (Qiagen, Germantown, MD) into water and then used directly for transcription as described above using a T3 mMessage mMachine kit. Primer sequences and construct amino acid sequences are included in Table S1.

Oocytes and electrophysiology

Whole *Xenopus laevis* ovaries were sourced from *Xenopus* I (Ann Arbor, MI) and cultured in ND98 (98 mM NaCl, 2 mM KCl, 1.8 mM $CaCl_2$, 1 mM $MgCl_2$, 5 mM HEPES, 2.5 mM Na-pyruvate, 100U/ml / 100mg/ml / 50 mg/ml of penicillin / streptomycin / tetracycline, pH 7.2. Tetracycline is a key addition for eliminating occasional bad batches of oocytes in the summer. Oocytes were released from the ovaries and defolliculated using 0.5-2 mg/ml Type II Collagenase in calcium-free antibiotic-free ND98 and gentle agitation on a rotary shaker. Two-electrode voltage clamp recordings were made in low Cl- ND96 (98 mM Na-methane sulfonate (MES), 1 mM $CaCl_2$, 1 mM $MgCl_2$, 2 mM KCl, 5 mM HEPES, pH 7.2) under 0.5-2 ml/min flow at room temperature (measured 20-22ºC). Borosilicate glass recording electrodes were filled with 3 mM KCl (0.5-1 MΩ) and bath pellet electrodes were isolated with an agarose bridge. Data was collected using a CA-1B amplifier (Dagan Instruments, Minneapolis, MN), and the pCLamp 10/Digidata 1440A acquisition system (Molecular Devices, Sunnyvale, CA). Data were digitized at 4-10 KHz and low pass filtered at 5 KHz. Isochronal tail currents were fit to a single Boltzmann for voltage-activation (GV) data, calculated for each recording using the equation: $G(V) = \left[\left(A_1 - A_2\right) / \left(1 - e^{\left(V - V_{50}\right)/s}\right)\right] + A_2$, where *G(V)* is the conductance at voltage *V*, A_1 is the minimum, A_2 is the maximum, *s* is the slope factor, and V_{50} is the midpoint of the curve. Data were analyzed using Clampfit (Molecular Devices) and OriginLab (Northhampton, MA). All chemicals for oocyte culture and electrophysiology were sourced from Sigma-Aldrich (Burlington, MA).

Structural Modelling

Structural models of the MlShak4 T1 (amino acids 112-197) and the MlShak5 T1 (amino acids 54-139) were generated using AlphaFold v2.1.0 (47) using default parameters, with top hits to a voltage-gated potassium channel (PDB: 2R9R). Tetramers were assembled from monomers by applying the rotational matrix from the Aplysia Kv1.1 T1 domain structure in VMD v. 1.9.4a55 (19,48). Protein structure files were generated for each model and solvated using the AutoPSF plugin and CHARMM36 force field (49). 10 nanosecond molecular dynamics simulations were performed using NAMD v.2.14 (50). To identify polar bonds, we used the native hydrogen bonds and salt bridges plugins in VMD. Hydrogen bonds were calculated within an acceptor-donor distance of 3.5 Å and angle cutoff of 20°, and salt bridges were calculated at

a distance of 4 Å. Fractional occupancy of each bond was calculated by dividing the number of frames that the interacting atoms were within the cutoff distance by the total number of frames in the simulation.

RESULTS

We scanned Shaker channel sequences from the ctenophore *Mnemiopsis leidyi* compiled by Li et al, 2015 (16) for N-terminal sequences with chemical similarity to known Shaker inactivation balls; a short flexible hydrophobic/neutral stretch of amino acids followed by a region including charges (10). We made expression vectors for three of the sequences with N-termini that matched this chemical profile, named MlShak3-5 here (*Mnemiopsis* protein IDs ML07807a, ML10392a and ML141713a, respectively) following the naming convention established in Li et al., 2015 (16) for MlShak1 and MlShak2. The MlShak3-5 N-termini are compared to characterized intrinsic Shaker subfamily inactivation balls and evolutionarily independent Kvβ, Shal and Shaw inactivation balls in Fig 2. Note that while N-type Inactivation ball sequences are conserved at the level of general chemical character, there is very little conservation at the level of sequence identity (Fig. 2), even between sea anemone (NvShak1) and jellyfish (jShak1) orthologs that have almost identical N-type inactivation properties (33,35). None of the three putative *Mnemiopsis* inactivation balls share significant sequence conservation, despite the fact that MlShak3 and MlShak4 are each other's closest phylogenetic relatives among all *Mnemiopsis* Shaker channels (16) and share ~ 54% amino acid identity across the T1/VSD/PD channel core. Note that there are > 40 Shaker-like channels in the *Mnemiopsis* genome and we do not intend to represent these three channels as the only MlShaks with the potential for N-type inactivation; these are just a sampling of good candidates based on cursory sequence analysis.

Fig. 3A-D shows families of outward K^+ currents recorded in response to 150 ms depolarizing steps from oocytes expressing MlShak3-5 compared to the N-type inactivating cnidarian N-type Shaker channel NvShak1. Two of the three *Mnemiopsis* channels, MlShak4 and MlShak5, show rapid inactivation like NvShak1, while MlShak3 inactivation is ~ 2 orders of magnitude slower. It is noteworthy that MlShak5 inactivates completely with a remaining pedestal current of < 1% of the peak current (n=8), whereas MlShak4 has a large pedestal current of 23 ± 4.5 (s.d.) % (n=9) at +50 mV remaining after N-type inactivation. To test whether inactivation in MlShak4 and MlShak5 is indeed N-type, we next made N-terminal deletion mutants for each (MlShak4Δ1-19, MlShak5Δ1-18) removing the putative inactivation ball sequences shown in Fig. 2. Currents recorded from oocytes expressing these two truncation mutants lack fast inactivation (Fig. 3E,F), demonstrating that the N-termini of MlShak4 and MlShak5 do indeed function as N-type inactivation balls. We did not examine the characteristics or mechanism of MlShak3 inactivation further in this study because it is clearly not a functional ortholog of classical rapidly inactivating N-type Shakers like NvShak1 or Shaker B.

We examined the voltage-dependence of activation for MlShak3-5 by measuring isochronal tail currents after 500 ms depolarizing prepulses of increasing voltage (Fig. 3G). For MlShak4 and MlShak5, we measured voltage-activation of the N-terminal deletion constructs as the rapid inactivation of the wild-type channels interfered with data collection. Data are shown with a simulated single Boltzmann fit. The voltage-activation ranges of these channels were typical for metazoan Shaker channels, resembling low-threshold cnidarian channels that exhibit N-type inactivation, with V_{50} values ranging from ~-25 mV to -5 mV (Fig. 3G) (35). It is possible that channels with higher activation thresholds and N-type inactivation, like those found in cnidarians and bilaterians (33,35), exist in ctenophores but were not captured in our sampling of channels.

Inactivation time constants (τ_{inact}) for MlShak4 and MlShak5 were measured using exponential fits of the inactivation time course (Fig. 4A). MlShak5 currents fit well with a single exponential, but MlShak4 currents benefitted from a double exponential fit due to a sloped baseline. We report just the large fast component of the fit as τ_{inact} for MlShak4 because it is the component selectively removed by N-terminal truncation (Fig. 3E). Inactivation time constants at a range of voltages are shown in Fig. 4B and are quantitatively similar to time constants reported for N-type inactivation in cnidarian N-type Shakers and *Drosophila* Shaker B from whole oocytes (33,35). Recovery from inactivation in MlShak4 and MlShak5 (Fig. 4C,D) is markedly slow with a Tau_{rec} of 551 +/- 116 (s.d.) ms (n=9)and 2822 +/- 454 (s.d.) ms (n=8) measured at -100 mV, respectively. The recovery time course of MlShak5 fit well with a single exponential while recovery for MlShak4 had fast and slow components. Here we show only a single exponential fit of the faster partial component for MlShak4; the slow component was more variable and impractical to quantify. In both cases, recovery is very slow compared to Shaker B which has a Tau_{rec} of ~50 ms (24). There is a precedent for slow recovery of N-type inactivation in mammalian Kv3.4 (51) and jellyfish Shalγ1 (34), and jShak1 recovery has both fast and slow components (33). Here, we will use the slow recovery to simplify calculations of the inactivation rate constant (k_{inact}, see below). Recovery rate positively correlates with pedestal current size, but the slow recovery we observe for MlShak4 indicates that recovery from inactivation is not responsible for its unusually large observed pedestal currents. We did not examine the underlying cause further in this study.

A key prediction for N-type inactivation is that the inactivation rate will be linearly proportional to the number of inactivation balls/channel. For Shaker B, the inactivation time constant and rate for channels with 1 inactivation ball is > 3.5x slower than the rate for WT channels (24). We co-expressed WT and truncated subunits in various ratios for both MlShak4 and MlShak5 to vary the average number of inactivation balls/channel to test if their inactivation obeys this prediction. The average number of inactivation balls/channel (N_{inact}) for any oocyte expressing WT and truncated forms can be predicted using a 4th power binomial expansion (Eq.

Eq. 1 $$(p+q)^4 = p^4 + 4p^3q + 6p^2q^2 + 4pq^3 + q^4$$

Eq. 2 $$N_{inact} = \left[4\left(p^4\right) + 3\left(4p^3q\right) + 2\left(6p^2q^2\right) + 4pq^3\right] / \left(1 - q^4\right)$$

1 and Eq. 2) where p = the frequency of WT subunits with a ball, q = the frequency of truncated subunits without a ball, and $p + q = 1$ (24). To calculate N_{inact}, each term in the binomial expansion is weighted by the number of inactivation balls they represent, and the sum is divided by the fraction of channels with N-type inactivation (Eq. 2). The value of q can be calculated from the magnitude of the non-inactivating or slowly inactivating current left after rapid N-type inactivation which represents q^4, the fraction of channels with no inactivation balls (Eq. 1). In a channel like MlShak5 that has essentially complete N-type inactivation, the residual steady state current in a MlShak5 WT + MlShak5 Δ2-18 co-expression mix should provide a direct, accurate measure of q^4, allowing easy derivation of q itself (Eq. 3). Because inactivation of WT MlShak4 is not complete, we had to use Eq. 4 to calculate q, accounting for the 23% fraction of the WT current that does not inactivate rapidly. In these equations, I_{ss} is the "steady state" or slowly inactivating current remaining after the rapid phase of N-type inactivation, and I_{inact} is the current fraction with rapid N-type inactivation. With q (and thus also p) in hand, the average number of

Eq. 3 $$q = \left(I_{SS}\, fraction\right)^{1/4}$$

Eq. 4 $$q = \left[\left(\left(I_{SS}\, fraction\right) - 0.23\right) / 0.77\right]^{1/4}$$

inactivation balls/channel contributing to I_{INACT} could be calculated for each oocyte using Eq. 1. Mackinnon et al. (1993) used this mathematical approach to predict for Shaker B that while k_{inact} should slow 4-fold, tau_{inact} should only slow ~3.5-fold in the transition from 4 to 1 inactivation ball because of the influence of rapid recovery from inactivation, and their experimental data from WT + N-terminal truncated channel mixes closely matches this prediction (24). For MIShak4 and MIShak5 which have extremely slow recovery from inactivation (Fig. 4C,D), the tau_{inact} for N-type inactivation should depend only on the rate constant of inactivation (k_{inact}) for a single inactivation ball multiplied by the number of inactivation balls (see Eq. 5 and Eq. 6 for examples of 4 and 1 inactivation ball, respectively). We can therefore predict that tau_{inact} should increase 4-fold as the I_{ss} fraction

Eq. 5 $$tau_{inact} = \left(4 \cdot k_{inact}\right)^{-1}$$

Eq. 6 $$tau_{inact} = \left(k_{inact}\right)^{-1}$$

increases. Fig. 5A,B show example traces recorded in response to +50 mV steps from a holding potential of -100 mV for WT compared to WT + truncated channel mixes for MIShak4 and MIShak5. Note the slowing of fast inactivation for both channels as the I_{ss} fraction increases. We used MIShak4 WT and MIShak5 to derive k_{inact} values of 73 +/- 13 (s.d.) s^{-1} (n=9) and 95 +/- 20 (s.d.) s^{-1} (n=8) at +50 mV, respectively. Fig. 5C,D show scatter plots of the fold change in tau_{inact} vs. I_{ss} fraction for varying ratios of MIShak4 WT + MIShak4 Δ2-19 and MIShak5 WT + MIShak5 Δ2-18, respectively. The curves show predictions for the fold change in tau_{inact} using WT k_{inact} and the predicted number of inactivation balls. For MIShak4, measured tau values from mixes closely match the predicted curve, as was previously found for *Drosophila* Shaker B and supports an identical mechanism in which each inactivation ball operates independently (24). MIShak5 tau_{inact} also slows significantly slows as I_{ss} fraction increases but approaches an ~3-fold change vs. the predicted 4-fold change. We speculate that this discrepancy arises from difficulty in accurately measuring tau_{inact} at higher I_{ss} fractions due to overlap of inactivation with the unusually slow activation time course MIShak5 (Fig. 3E). Alternatively, a small amount of negative cooperativity due to steric hindrance might explain the discrepancy. Regardless, both MIShak4 and MIShak5 meet the expectation for N-type inactivation that tau_{inact} should depend on the number of inactivation balls. Furthermore, the time course for recovery from N-type inactivation should be independent of the number inactivation balls, and we saw no change in recovery rate as I_{SS} fraction varied for either channel (Fig. 5E,F).

We next swapped inactivation balls between MIShak4 and MIShak5 to see if they show promiscuous block as has been observed between bilaterian Shaker family channels (44-46). We replaced amino acids 2-19 in MIShak4 with 2-18 of MIShak5, and amino acids 2-18 of MIShak5 with 2-19 of MIShak4 (see Table S1 for chimeric channel sequences). Both chimeric channels inactivate fully (Fig. 6A-D), demonstrating cross compatibility for the inactivation balls. Inactivation is slowed ~8-fold with the MIShak5 ball and the MIShak4 pore compared to MIShak5 WT, but the MIShak4 ball on the MIShak5 pore inactivates at a similar speed to the two WT channels. The lack of a pedestal current in either chimera suggests the large pedestal current of MIShak4 derives from the specific interaction between its ball and receptor rather than being an intrinsic feature of either one. We were surprised to see that despite this cross-compatibility demonstrated with chimeric channels, tau_{inact} did not increase as expected with increasing ISS fraction when we mixed MIShak5 WT with MIShak4 Δ2-19 in varying ratios (Fig. 6E,F). We interpret this to mean that the number of inactivation balls did not change for N-type inactivating channels in this mix. This result is explainable only if MIShak4 and MIShak5 do not form heteromultimers. If the channels assemble independently, varying the expression ratio would vary the abundance but not subunit/inactivation ball stoichiometry of N-type inactivating channels (MIShak5).

To gain further insights into the potential for heteromerization between MlShak4 and MlShak5, we built structural models of tetrameric T1 assembly domain rings for MlShak4 homomers, MlShak5 homomers and 2:2 MlShak4:MlShak5 heteromers. We modeled the tetrameric T1 ring in isolation for computational efficiency since it is well established that T1s can tetramerize when expressed in isolation. The cytoplasmic T1 assembly domain specifies subfamily-specific assembly at the level of the polar bonds which can form along T1-T1 interfaces (19,52-55). T1 ring assembly occurs co-translationally (56,57), is the first step in tetrameric channel assembly and greatly enhances assembly as measured by surface expression. For these reasons, it is expected to play a dominant role in determining the subunit composition of functional tetrameric Shaker family channels. Homomeric MlShak4 and MlShak5 T1 rings form several hydrogen bonds and salt bridges across the entire T1:T1 interface (Fig. 7A,B), comparable to the distribution and number of bonds seen in the tetrameric T1 crystal structure of Aplysia Kv1.1 (Table 1) (19). In contrast, T1 interfaces between MlShak4 and MlShak5 in the 2:2 heteromer model formed only a few isolated polar bonds (Fig. 7C,D), many of which had notably lower occupancy than in the homomeric models (Table 1), suggesting the ring is likely to be far less stable. Several of the binding residues are not conserved between MlShak4 and MlShak5 (e.g. E66 in MlShak5 is I24 in MlShak4), and furthermore, conserved binding residues do not always interact in the same way in different Kv subfamilies because of changes in the surrounding context (55). Mutations that disrupt polar T1-T1 polar bonding observed in structures have been demonstrated to reduce tetramer formation (52,53,55). Thus, these molecular dynamics simulations suggest the independent assembly of MlShak4 and MlShak5 as we observe in co-expression experiments likely occurs because of T1 incompatibility.

DISCUSSION

We conclusively show here that N-type fast inactivation is present in a subset of Shaker channels in the ctenophore *Mnemiopsis leidyi*. The widespread functional conservation of fast N-type inactivating Shakers (N-type Shakers) in both cnidarians and bilaterians coupled with their presence in a ctenophore, as shown here, implies that N-type Shakers were present in the last common ancestor of all modern animals. Nevertheless, given that N-type inactivation has evolved independently multiple times within various animal lineages (10,34) and molecular phylogenies showed that Shakers independently diversified within these major animal lineages (16,17,33-35,58), we can't completely rule out the possibility that the N-type Shakers of cnidarians, bilaterians, and ctenophores arose independently. However, within cnidarians, N-type Shakers evolved early; the gene encoding NvShak1 can be traced in phylogenies to the common cnidarian ancestor and NvShak1 orthologs show rapid inactivation in multiple cnidarian lineages, suggesting continuous conservation of an ancestral N-type phenotype in this gene across Cnidaria (33,35,43). It is also intriguing that *Nematostella vectensis* orthologs with proven N-type inactivation (NvShak1,4,5) form a clade in gene phylogenies (17). Still, there is not sufficient N-terminal conservation or functional data from diverse species to conclude that the phenotype has been evolutionarily conserved across this broader cnidarian clade. Similarly, in bilaterians, the widespread presence of a single Shaker channel with fast inactivation in protostome invertebrates suggests the ancestral protostome Shaker probably had N-type inactivation. However, in deuterostomes the lack of functional data on Shakers from species outside of Vertebrata such as echinoderms and tunicates making it difficult to infer the state of N-type inactivation in the Shaker channels of key ancestral nodes within Deuterostomia. Functional characterization of Shaker α-subunits and β-subunits from echinoderms and tunicates and lancelets will shed light on whether on the evolutionary conservation of N-type inactivation in the deuterostomes and whether there has been evolutionary conservation of N-

type Shakers despite the change in the source of the inactivation ball from α to β subunits in vertebrates (37). Expanding the taxonomic coverage of functional analyses on Shakers would provide key insights into the origin(s) and early evolution of the N-type Shaker phenotype across the breadth of the animal tree.

We should also note that there is considerable evidence for non-inactivating or slowly inactivating Shakers in animal ancestor as well. Cnidarians and bilaterians both have Shakers lacking fast inactivation (35,59,60), and we show the same for ctenophores with MlShak3 here. Even *Drosophila* Shaker encodes multiple variants with highly variable inactivation mechanisms and rates via N-terminal and pore splicing (61,62). Furthermore, while previously expressed *Mnemiopsis* Shakers MlShak1 and MlShak2 do not form functional homomeric channels, they do heteromerize with delayed-rectifier type cnidarian and bilaterian Shakers (16) and the heteromeric channels lack fast inactivation. Thus, Shaker channels that lack fast inactivation have a similar phylogenetic spread to N-type Shakers.

One of the more intriguing and unexpected aspects of Shaker gene family evolution in animals is that the family as a whole, and Shaker subfamily in particular, is greatly expanded in ctenophores and cnidarians relative to bilaterians. Phylogenetic analysis points to at least 23 Shaker family (and 12 Shaker subfamily) genes in the common cnidarian ancestor compared to 4 Shaker family genes and 1 Shaker subfamily gene predicted for the common bilaterian ancestor (17). Shaker complexity in the ctenophore ancestor has not yet been assessed, but *Mnemiopsis leidyi* has > 40 Shaker or Shaker-like genes (16), and their high sequence diversity suggests the gene duplications that produced them are ancient. These Shaker channels represent the large majority of voltage-gated K^+ diversity in *Mnemiopsis*; there are no Shab, Shal or Shaw channels (16), no KCNQ channels (16) and only two other Eag-like channels (63). It is entirely possible that ancestral metazoans also had multiple Shaker subfamily genes, the presence of which is obscured in phylogenies based on extant species by sequence divergence and/or gene losses over evolutionary time.

The adaptive advantage that N-type Shakers conferred on early animals isn't entirely clear because the specific role of N-type inactivation in Shakers in electrical signaling has not been extensively explored. There are studies, including one from Dr. Aldrich, showing that rapid K^+ channel inactivation results in frequency-dependent action potential broadening (64,65), but this physiological role has not specifically been associated with N-type Shakers at a genetic level. There are a couple of additional possibilities to speculate on. First, N-type Shakers might simply allow a higher action potential firing rate than slowly inactivating Shakers by limiting the duration of the late K^+ conductance. The presence of multiple Shaker inactivation phenotypes in early animals could have allowed for neurons with distinct intrinsic firing rates. Second, N-type Shakers in muscle cells could allow for partial repolarization to provide driving force for Ca^{2+} entry, provided other K^+ channels are present to complete delayed repolarization. This is the role I_{to} plays in cardiac myocytes (66), though the inactivation rates of the underlying channels (Kv1.4/Kv4.2/Kv4.3) are slower than the classical N-type inactivation we discuss here.

The inability of MlShak4 and MlShak5 to form heteromeric channels is extremely interesting because one might have predicted that *Mnemiopsis* Kv channels would be universally cross-compatible given their affinity for the Shaker (Kv1) subfamily in phylogenies (16). Furthermore, all *Mnemiopsis* Shakers lack the T1 interface Zn^{2+} binding site that distinguishes the Shab (Kv2), Shaw (Kv3) and Shal (Kv4) subfamilies from Shaker (55), suggesting structural similarity in *Mnemiopsis* Shaker T1s. However, the assembly incompatibility we find here for MlShak4 and MlShak5 raises the possibility that ctenophores might have nevertheless independently evolved their own unique gene subfamilies to allow for expression of multiple distinct Shaker channels in the same cells. In addition, the inability of MlShak1 and MlShak2 to form functional homomeric channels is reminiscent of cnidarian and bilaterian "silent" or "regulatory" subunits that assemble only as heteromers (16,17,34,35,67-70). Both results suggest active evolution of subunit compatibility within the ctenophore Shaker

subfamily. A broad functional characterization of *Mnemiopsis* Shakers coupled with evolutionary analysis of Shaker conservation across diverse ctenophore species will help determine if ctenophores did indeed have their own set of assembly-exclusive gene subfamilies evolved from within the broader Shaker subfamily umbrella. We show here that structural modeling of T1 assembly domain interactions when combined with co-expression experiments is a powerful tool for identifying these Shaker assembly phenotypes and their underlying molecular basis.

FIGURE LEGENDS

Figure 1. Mechanism and Phylogenetic distribution of N-type Inactivation. A) Each subunit of a homotetrameric N-type inactivating Shaker channel has an inactivation "ball" that can block the channel pore after it opens. However only a single inactivation ball can occupy the pore binding site at any one time. B) Animal phylogeny overlaid with current knowledge for the presence or absence and inactivation phenotypes of Shaker channels. Placozoans and sponges lack recognizable nervous systems and sponges are the only major lineage lacking Shaker. Question marks signify that the inactivation phenotypes of Shakers from ctenophores, placozoans and invertebrate deuterostomes (echinoderms and tunicates) are unknown. Here we functionally characterize ctenophore Shakers to gain insights into possible Shaker inactivation phenotypes in the animal last common ancestor (LCA).

Figure 2. N termini of MlShak3-5 compared to amino acid sequences of Kv channel N-terminal inactivation balls. Only the first 20 amino acids are shown because a Shaker B peptide covering this region is sufficient to reconstitute N-type inactivation in truncated channels (46). The top block shows MlShak3-5, the middle block is Shaker subfamily channels with intrinsic inactivation balls and the bottom block is other Kv subunit inactivation balls. Amino acids are highlighted by chemical characteristics: light green = small, flexible, uncharged; dark green = large, hydrophobic; blue = positively charged; burnt orange = negatively charged; grey = larger polar. Numbers on the right side of sequences represent the length of the chain connecting the N-terminus shown here to the conserved channel core (T1 domain).

Figure 3. N-type inactivation in ctenophore Shaker channels. (A-F) Example current traces from whole oocytes recorded under two-electrode voltage clamp in response to 150 ms depolarization steps from -50 mV to 50mV in 20-mV increments from a holding potential of -100 mV. Panels show (A) *Nematostella vectensis* NvShak1 as an example of classic rapid N-type inactivation (B) MlShak3, (C) MlShak4, (D) MlShak5, (E) MlShak4 Δ1-19, and (F) MlShak5 Δ1-18. (G) Normalized voltage-activation (GV) relationships for wild-type MlShak3 and N-terminal truncated MlShak4 and MlShak5. GV curves were calculated from isochronal tail currents recorded at -20mV after 500 ms depolarizing steps from ranging from -70 mV to +70 mV in 10-mV increments. MlShak3 V_{50} = -5.6 ± 4.0 (s.d) mV and slope = 16.8 ± 1.1 (s.d) mV (n=10); MlShak4 Δ2-18 V_{50} = -20.5 ± 3.2 (s.d) mV and slope = 11.9 ± 0.9 (s.d) mV (n=11); MlShak5 V_{50} = -25.1 ± 1.9 (s.d) mV and slope = 8.4 ± 0.8 (s.d) mV (n=9). Error bars show standard deviation from the mean. Data were averaged for display after normalization.

Figure 4. Characterization of the N-type inactivation properties of MlShak4 and MlShak5. (A) For fitting the time course of inactivation, currents were elicited with 500 ms depolarizing steps from -50 mV to 70 mV in 10 mV-increments (holding at -100 mV, tail at -100 mV) (inset). Example current traces for MlShak4 and MlShak5 elicited by a step to 50 mV are shown with double and single exponential fits of fast inactivation overlayed (gray lines), respectively. (B) Fast inactivation time constants for MlShak4 (n=9) and MlShak5 (n=8) at the indicated voltages. Data point show mean ± standard deviation. (C) Example traces for recovery from inactivation

for MlShak4. Recovery was determined using two 500 ms steps to 50mV separated by a recovery step to -100 mV ranging from 70 ms to 970 ms in 50 ms increments. The first step was used to induce inactivation and recovery was measured from peak currents in the 2nd step (graph). Data shown in the graph is from a single oocyte, but the reported tau_{rec} is the mean ± S.D. from 10 oocytes. Oocytes were held at -100 mV for 18 s between sweeps to allow for full recovery. (D) Recovery example for MlShak5. For MlShak5, recovery steps to -100 mV ranged from 500-9500 ms in 500 ms increments, the interpulse holding time at -100 mV was 25 s, and the reported tau_{rec} is the mean ± S.D. of measurements from 10 oocytes.

Figure 5. Time constant of N-type inactivation in MlShak4 and MlShak5 depends on the number of inactivation balls. (A,B) Example traces of WT MlShak4 and MlShak5 currents (gray traces) compared to currents from oocytes co-expressing MlShak4 WT + MlShak4 Δ2-19 and MlShak5 WT + MlShak5 Δ2-18 (black traces), respectively. Currents were elicited by 150 ms depolarizations to 50 mV from a holding potential of -100 mV and are normalized by peak current magnitude. Insets show traces normalized to both peak current and pedestal current to highlight the differences in the time course of fast inactivation. (C,D) Graphs of tau_{inact} vs. fraction of non-inactivating current for mixes of MlShak4 WT + MlShak4 Δ2-19 and MlShak5 + MlShak5 Δ2-18 at varying ratios. Currents were elicited by 150 ms steps to 50 mV from a holding potential of -100 mV and fit as shown in Fig. 4A,B. We normalized tau_{inact} for each oocyte to tau_{inact} for the respective WT channel to show fold change in the inactivation time course, and each data point represents a single oocyte. The smooth curves show the predicted tau_{inact} for the expected average number of inactivation balls at the indicated fraction of non-inactivating current as described in the text. (E,F) Normalized recovery time constants (tau_{rec} mix/tau_{rec} WT) for WT + N-terminal truncated channels mixed at various ratios show that the time course of recovery is not sensitive to the number of inactivation balls. Recovery was determined as in Fig. 4C,D) and measurements were made from the same oocytes as shown in panels C,D, although we did not successfully document recovery from all of them.

Figure 6. MlShak4 and MlShak5 inactivation balls cross-react but indicate these channels do not co-assemble. (A,B) Example traces and graph of tau_{inact} vs. voltage for a chimeric MlShak4 channel where the inactivation ball has been replaced with the inactivation ball of MlShak5. The voltage protocols were as described in Fig. 4A,B and the data in the graph shows mean ± S.D. from 8 oocytes. (C,D) Similar data for a chimeric channel with the MlShak4 inactivation ball replacing the intrinsic inactivation ball of MlShak5. Recovery time constants were also calculated as shown in Fig. 4C,D) for MlShak5 ball + MlShak4 pore (n=8) and MlShak4 ball + MlShak5 pore (n = 8) (tau_{rec} = 1141 ± 191 (s.d.) ms and 1043 ± 204 (s.d.) ms, respectively), but are not shown here. (E) Example trace (black) from an oocyte expressing a mixture of MlShak5 WT + MlShak4 Δ 2-19 compared to MlShak5 WT (solid gray) and a mixture of MlShak WT + MlShak5 Δ 2-18 (dotted gray); traces are normalized by peak current. Inlay shows traces normalized to both peak and pedestal current for clearer comparison of the time course of fast inactivation. (F) Normalized tau_{inact} (to tau_{inact} of MlShak5 WT) for oocytes expressing varying ratios of MlShak5 WT + MlShak4 Δ 2-19 plotted vs. the fraction of non-inactivating current. Note there was no dependence of tau_{inact} on the ratio, suggesting the number of inactivation balls on channels in the inactivating fraction does not change as the mix of channels varies.

Figure 7. Interactions between the T1 assembly domains for MlShak4 and MlShak5. T1-T1 interface polar bonds in tetrameric T1 rings for an MlShak4 homomer (A), an MlShak5 homomer (B) and right and left sides in a 2:2 MlShak4:MlShak5 heteromer. Polar Interacting residues identified from a 10 ns molecular dynamics simulation are highlighted green and labeled. Bonds

are shown as dotted lines with line thickness scaled to fractional occupancy. Hydrogen bonds are represented by black lines, and salt bridges are represented by red lines. The homomeric interfaces of (A) MlShak4 and (B) MlShak5 exhibited notably more bonds (6-7 unique interactions) than either of the heteromeric interfaces (3-4 unique bonds) (C-D). See Table 1 for a comprehensive list of bond occupancies.

Table 1. Occupancy of T1-T1 interactions

MlShak4			**MlShak5**			**MlShak4-MlShak5**			**MlShak5-MlShak4**		
Left	Right	Occupancy	Left	Right	Occupancy	Left	Right	Occupancy	Left	Right	Occupancy
T125	D157	0.96	K63	Q103	0.75	**D164**	**K63**	0.63	**E66**	**R122**	0.44
T129	D157	0.71	**E66**	**R122**	0.94	Q171	D100	0.53	T67	D157	0.74
D164	**R160**	0.98	**E66**	**K94**	0.98	Y177	N102	0.54	Q114	D157	0.49
Y168	E189	0.84	T67	D157	0.94				Q114	R160	0.73
Q171	R160	0.89	Y111	E132	0.68						
Q177	E183	0.75	Q114	D157	0.84						
			Y120	N102	0.56						
	Total	**5.11**		**Total**	**5.69**		**Total**	**1.71**		**Total**	**2.40**

Pairs of interacting polar residues and their fractional occupancy are listed for homomeric and heteromeric combinations of MlShak4 and MlShak5 T1 domains as determined from molecular dynamics simulations (See Fig. 7 for details). Bolded residues indicate salt bridge interactions and regular text indicates hydrogen bonds. The sums of occupancies are shown at the bottom.

AUTHOR CONTRIBUTIONS

B.T.S. and T.J. conceived and designed the experiments. B.T.S. performed bioinformatics and electrophysiology experiments and data analyses. M.J. performed bioinformatics experiments. J.F.R. provided reagents. B.T.S and T.J. wrote the initial manuscript and all authors contributed to editing.

ACKNOWLEDGEMENTS

We dedicate this manuscript to Rick Aldrich, whose scientific achievements and fabulous mentoring directly inspired it. Funding: This work was supported by the Huck Institutes for the Life Sciences (T.J), Penn State Department of Biology (T.J.), a National Science Foundation award (DEB-1542597, J.F.R.) and an Allen Distinguished Investigator Award, a Paul G. Allen Frontiers Group advised grant of the Paul G. Allen Family Foundation (J.F.R).

DECLARATION OF INTERESTS

The authors declare no competing interests.

REFERENCES

1. Hodgkin, A. L., and A. F. Huxley. 1952. A quantitative description of membrane current and its application to conduction and excitation in nerve. *J Physiol*. 117(4):500-544, doi: 10.1113/jphysiol.1952.sp004764.

2. Armstrong, C. M., and F. Bezanilla. 1977. Inactivation of the sodium channel. II. Gating current experiments. *J Gen Physiol*. 70(5):567-590, doi: 10.1085/jgp.70.5.567.

3. Armstrong, C. M., F. Bezanilla, and E. Rojas. 1973. Destruction of sodium conductance inactivation in squid axons perfused with pronase. *J Gen Physiol*. 62(4):375-391, doi: 10.1085/jgp.62.4.375.

4. Fernández-Mariño, A. I., X. F. Tan, C. Bae, K. Huffer, J. Jiang, and K. J. Swartz. 2023. Inactivation of the Kv2.1 channel through electromechanical coupling. *Nature*. 622(7982):410-417, doi: 10.1038/s41586-023-06582-8.

5. Ye, W., H. Zhao, Y. Dai, Y. Wang, Y. H. Lo, L. Y. Jan, and C. H. Lee. 2022. Activation and closed-state inactivation mechanisms of the human voltage-gated K(V)4 channel complexes. *Mol Cell*. 82(13):2427-2442.e2424, doi: 10.1016/j.molcel.2022.04.032.

6. Zagotta, W. N., T. Hoshi, and R. W. Aldrich. 1990. Restoration of inactivation in mutants of Shaker potassium channels by a peptide derived from ShB. *Science*. 250(4980):568-571, http://www.ncbi.nlm.nih.gov/pubmed/2122520.

7. Hoshi, T., W. N. Zagotta, and R. W. Aldrich. 1990. Biophysical and molecular mechanisms of Shaker potassium channel inactivation. *Science*. 250(4980):533-538, http://www.ncbi.nlm.nih.gov/pubmed/2122519.

8. Hoshi, T., W. N. Zagotta, and R. W. Aldrich. 1991. Two types of inactivation in Shaker K+ channels: effects of alterations in the carboxy-terminal region. *Neuron*. 7(4):547-556, doi: 0896-6273(91)90367-9 [pii], http://www.ncbi.nlm.nih.gov/pubmed/1931050.

9. Tan, X. F., C. Bae, R. Stix, A. I. Fernández-Mariño, K. Huffer, T. H. Chang, J. Jiang, J. D. Faraldo-Gómez, and K. J. Swartz. 2022. Structure of the Shaker Kv channel and mechanism of slow C-type inactivation. *Science advances*. 8(11):eabm7814, doi: 10.1126/sciadv.abm7814.

10. Sukomon, N., C. Fan, and C. M. Nimigean. 2023. Ball-and-Chain Inactivation in Potassium Channels. *Annu Rev Biophys*. 52:91-111, doi: 10.1146/annurev-biophys-100322-072921.

11. Tempel, B. L., D. M. Papazian, T. L. Schwarz, Y. N. Jan, and L. Y. Jan. 1987. Sequence of a probable potassium channel component encoded at Shaker locus of Drosophila. *Science*. 237(4816):770-775, http://www.ncbi.nlm.nih.gov/pubmed/2441471.

12. Pongs, O., N. Kecskemethy, R. Muller, I. Krah-Jentgens, A. Baumann, H. H. Kiltz, I. Canal, S. Llamazares, and A. Ferrus. 1988. Shaker encodes a family of putative potassium channel proteins in the nervous system of Drosophila. *EMBO J*. 7(4):1087-1096, http://www.ncbi.nlm.nih.gov/pubmed/2456921.

13. Kamb, A., L. E. Iverson, and M. A. Tanouye. 1987. Molecular characterization of Shaker, a Drosophila gene that encodes a potassium channel. *Cell*. 50(3):405-413, doi: 0092-8674(87)90494-6 [pii], http://www.ncbi.nlm.nih.gov/pubmed/2440582.

14. Wei, A., T. Jegla, and L. Salkoff. 1996. Eight potassium channel families revealed by the C. elegans genome project. *Neuropharmacology*. 35(7):805-829, doi: 0028390896001268 [pii], http://www.ncbi.nlm.nih.gov/pubmed/8938713.

15. Salkoff, L., K. Baker, A. Butler, M. Covarrubias, M. D. Pak, and A. Wei. 1992. An essential 'set' of K+ channels conserved in flies, mice and humans. *Trends in neurosciences*. 15(5):161-166, http://www.ncbi.nlm.nih.gov/pubmed/1377421.

16. Li, X., H. Liu, J. Chu Luo, S. A. Rhodes, L. M. Trigg, D. B. van Rossum, A. Anishkin, F. H. Diatta, J. K. Sassic, D. K. Simmons, B. Kamel, M. Medina, M. Q. Martindale, and T. Jegla. 2015. Major diversification of voltage-gated K+ channels occurred in ancestral parahoxozoans. *Proc Natl Acad Sci U S A*. 112(9):E1010-1019, doi: 10.1073/pnas.1422941112.

17. Lara, A., B. T. Simonson, J. F. Ryan, and T. Jegla. 2023. Genome-Scale Analysis Reveals Extensive Diversification of Voltage-Gated K+ Channels in Stem Cnidarians. *Genome biology and evolution*. 15(3), doi: 10.1093/gbe/evad009.

18. Pfaffinger, P. J., and D. DeRubeis. 1995. Shaker K+ channel T1 domain self-tetramerizes to a stable structure. *J Biol Chem*. 270(48):28595-28600.

19. Kreusch, A., P. J. Pfaffinger, C. F. Stevens, and S. Choe. 1998. Crystal structure of the tetramerization domain of the Shaker potassium channel. *Nature*. 392(6679):945-948, doi: 10.1038/31978, http://www.ncbi.nlm.nih.gov/pubmed/9582078.

20. Long, S. B., E. B. Campbell, and R. Mackinnon. 2005. Crystal structure of a mammalian voltage-dependent Shaker family K+ channel. *Science*. 309(5736):897-903, doi: 10.1126/science.1116269.

21. MacKinnon, R. 1991. Determination of the subunit stoichiometry of a voltage-activated potassium channel. *Nature*. 350(6315):232-235, doi: 10.1038/350232a0, http://www.ncbi.nlm.nih.gov/pubmed/1706481.

22. Shen, N. V., and P. J. Pfaffinger. 1995. Molecular recognition and assembly sequences involved in the subfamily-specific assembly of voltage-gated K+ channel subunit proteins. *Neuron*. 14(3):625-633, doi: 0896-6273(95)90319-4 [pii], http://www.ncbi.nlm.nih.gov/pubmed/7695909.

23. Kobertz, W. R., C. Williams, and C. Miller. 2000. Hanging gondola structure of the T1 domain in a voltage-gated K(+) channel. *Biochemistry*. 39(34):10347-10352, doi: 10.1021/bi001292j.

24. MacKinnon, R., R. W. Aldrich, and A. W. Lee. 1993. Functional stoichiometry of Shaker potassium channel inactivation. *Science*. 262(5134):757-759, http://www.ncbi.nlm.nih.gov/pubmed/7694359.

25. dos Reis, M., Y. Thawornwattana, K. Angelis, M. J. Telford, P. C. Donoghue, and Z. Yang. 2015. Uncertainty in the Timing of Origin of Animals and the Limits of Precision in Molecular Timescales. *Current biology : CB*. 25(22):2939-2950, doi: 10.1016/j.cub.2015.09.066.

26. Peterson, K. J., J. A. Cotton, J. G. Gehling, and D. Pisani. 2008. The Ediacaran emergence of bilaterians: congruence between the genetic and the geological fossil records. *Philos Trans R Soc Lond B Biol Sci*. 363(1496):1435-1443, doi: 10.1098/rstb.2007.2233.

27. Peterson, K. J., J. B. Lyons, K. S. Nowak, C. M. Takacs, M. J. Wargo, and M. A. McPeek. 2004. Estimating metazoan divergence times with a molecular clock. *Proc Natl Acad Sci U S A*. 101(17):6536-6541, doi: 10.1073/pnas.0401670101.

28. Ryan, J. F., K. Pang, N. C. S. Program, J. C. Mullikin, M. Q. Martindale, and A. D. Baxevanis. 2010. The homeodomain complement of the ctenophore Mnemiopsis leidyi suggests that Ctenophora and Porifera diverged prior to the ParaHoxozoa. *EvoDevo*. 1(1):9, doi: 10.1186/2041-9139-1-9, http://www.ncbi.nlm.nih.gov/pubmed/20920347.

29. Ryan, J. F., K. Pang, C. E. Schnitzler, A. D. Nguyen, R. T. Moreland, D. K. Simmons, B. J. Koch, W. R. Francis, P. Havlak, N. C. S. Program, S. A. Smith, N. H. Putnam, S. H. Haddock, C. W. Dunn, T. G. Wolfsberg, J. C. Mullikin, M. Q. Martindale, and A. D. Baxevanis. 2013. The genome of the ctenophore Mnemiopsis leidyi and its implications for cell type evolution. *Science*. 342(6164):1242592, doi: 10.1126/science.1242592, http://www.ncbi.nlm.nih.gov/pubmed/24337300.

30. Moroz, L. L., K. M. Kocot, M. R. Citarella, S. Dosung, T. P. Norekian, I. S. Povolotskaya, A. P. Grigorenko, C. Dailey, E. Berezikov, K. M. Buckley, A. Ptitsyn, D. Reshetov, K. Mukherjee, T. P. Moroz, Y. Bobkova, F. Yu, V. V. Kapitonov, J. Jurka, Y. V. Bobkov, J. J. Swore, D. O. Girardo, A. Fodor, F. Gusev, R. Sanford, R. Bruders, E. Kittler, C. E. Mills, J. P. Rast, R. Derelle, V. V. Solovyev, F. A. Kondrashov, B. J. Swalla, J. V. Sweedler, E. I. Rogaev, K. M. Halanych, and A. B. Kohn. 2014. The ctenophore genome and the evolutionary origins of neural systems. *Nature*. 510(7503):109-114, doi: 10.1038/nature13400, http://www.ncbi.nlm.nih.gov/pubmed/24847885.

31. Schultz, D. T., S. H. D. Haddock, J. V. Bredeson, R. E. Green, O. Simakov, and D. S. Rokhsar. 2023. Ancient gene linkages support ctenophores as sister to other animals. *Nature*. 618(7963):110-117, doi: 10.1038/s41586-023-05936-6.

32. Li, Y., X. X. Shen, B. Evans, C. W. Dunn, and A. Rokas. 2021. Rooting the Animal Tree of Life. *Molecular biology and evolution*. 38(10):4322-4333, doi: 10.1093/molbev/msab170.

33. Jegla, T., N. Grigoriev, W. J. Gallin, L. Salkoff, and A. N. Spencer. 1995. Multiple Shaker potassium channels in a primitive metazoan. *J Neurosci*. 15(12):7989-7999, http://www.ncbi.nlm.nih.gov/pubmed/8613736.

34. Jegla, T., and L. Salkoff. 1997. A novel subunit for shal K+ channels radically alters activation and inactivation. *The Journal of neuroscience : the official journal of the Society for Neuroscience*. 17(1):32-44, http://www.ncbi.nlm.nih.gov/pubmed/8987734.

35. Jegla, T., H. Q. Marlow, B. Chen, D. K. Simmons, S. M. Jacobo, and M. Q. Martindale. 2012. Expanded functional diversity of shaker K(+) channels in cnidarians is driven by gene expansion. *PLoS One*. 7(12):e51366, doi: 10.1371/journal.pone.0051366 PONE-D-12-29489 [pii], http://www.ncbi.nlm.nih.gov/pubmed/23251506.

36. Heinemann, S., J. Rettig, V. Scott, D. N. Parcej, C. Lorra, J. Dolly, and O. Pongs. 1994. The inactivation behaviour of voltage-gated K-channels may be determined by association of alpha- and beta-subunits. *J Physiol Paris*. 88(3):173-180, doi: 0928-4257(94)90003-5 [pii], http://www.ncbi.nlm.nih.gov/pubmed/7833860.

37. Rettig, J., S. H. Heinemann, F. Wunder, C. Lorra, D. N. Parcej, J. O. Dolly, and O. Pongs. 1994. Inactivation properties of voltage-gated K+ channels altered by presence

of beta-subunit. *Nature*. 369(6478):289-294, doi: 10.1038/369289a0, http://www.ncbi.nlm.nih.gov/pubmed/8183366.

38. Kim, M., D. J. Baro, C. C. Lanning, M. Doshi, J. Farnham, H. S. Moskowitz, J. H. Peck, B. M. Olivera, and R. M. Harris-Warrick. 1997. Alternative splicing in the pore-forming region of shaker potassium channels. *J Neurosci*. 17(21):8213-8224, http://www.ncbi.nlm.nih.gov/pubmed/9334397.

39. Kim, E., T. A. Day, J. L. Bennett, and R. A. Pax. 1995. Cloning and functional expression of a Shaker-related voltage-gated potassium channel gene from Schistosoma mansoni (Trematoda: Digenea). *Parasitology*. 110 (Pt 2):171-180, doi: 10.1017/s0031182000063939.

40. Pfaffinger, P. J., Y. Furukawa, B. Zhao, D. Dugan, and E. R. Kandel. 1991. Cloning and expression of an Aplysia K+ channel and comparison with native Aplysia K+ currents. *J Neurosci*. 11(4):918-927, doi: 10.1523/jneurosci.11-04-00918.1991.

41. Santi, C. M., A. Yuan, G. Fawcett, Z. W. Wang, A. Butler, M. L. Nonet, A. Wei, P. Rojas, and L. Salkoff. 2003. Dissection of K+ currents in Caenorhabditis elegans muscle cells by genetics and RNA interference. *Proc Natl Acad Sci U S A*. 100(24):14391-14396, doi: 10.1073/pnas.1935976100 [pii], http://www.ncbi.nlm.nih.gov/pubmed/14612577.

42. Liu, Q., P. B. Kidd, M. Dobosiewicz, and C. I. Bargmann. 2018. C. elegans AWA Olfactory Neurons Fire Calcium-Mediated All-or-None Action Potentials. *Cell*. 175(1):57-70.e17, doi: 10.1016/j.cell.2018.08.018.

43. Bouchard, C., R. B. Price, C. G. Moneypenny, L. F. Thompson, M. Zillhardt, L. Stalheim, and P. A. Anderson. 2006. Cloning and functional expression of voltage-gated ion channel subunits from cnidocytes of the Portuguese Man O'War Physalia physalis. *J Exp Biol*. 209(Pt 15):2979-2989, doi: 10.1242/jeb.02314, http://www.ncbi.nlm.nih.gov/pubmed/16857882.

44. Ruppersberg, J. P., R. Frank, O. Pongs, and M. Stocker. 1991. Cloned neuronal IK(A) channels reopen during recovery from inactivation. *Nature*. 353(6345):657-660, doi: 10.1038/353657a0.

45. Stephens, G. J., D. G. Owen, A. Opalko, M. R. Pisano, W. H. MacGregor, and B. Robertson. 1996. Studies on the blocking action of human Kv3.4 inactivation peptide variants in the mouse cloned Kv1.1 K+ channel. *J Physiol*. 496 (Pt 1)(Pt 1):145-154, doi: 10.1113/jphysiol.1996.sp021672.

46. Murrell-Lagnado, R. D., and R. W. Aldrich. 1993. Interactions of amino terminal domains of Shaker K channels with a pore blocking site studied with synthetic peptides. *J Gen Physiol*. 102(6):949-975, doi: 10.1085/jgp.102.6.949.

47. Jumper, J., R. Evans, A. Pritzel, T. Green, M. Figurnov, O. Ronneberger, K. Tunyasuvunakool, R. Bates, A. Žídek, A. Potapenko, A. Bridgland, C. Meyer, S. A. A. Kohl, A. J. Ballard, A. Cowie, B. Romera-Paredes, S. Nikolov, R. Jain, J. Adler, T. Back, S. Petersen, D. Reiman, E. Clancy, M. Zielinski, M. Steinegger, M. Pacholska, T. Berghammer, S. Bodenstein, D. Silver, O. Vinyals, A. W. Senior, K. Kavukcuoglu, P. Kohli, and D. Hassabis. 2021. Highly accurate protein structure prediction with AlphaFold. *Nature*. 596(7873):583-589, doi: 10.1038/s41586-021-03819-2.

48. Humphrey, W., A. Dalke, and K. Schulten. 1996. VMD: visual molecular dynamics. *J Mol Graph*. 14(1):33-38, 27-38.

49. Huang, J., S. Rauscher, G. Nawrocki, T. Ran, M. Feig, B. L. De Groot, H. Grubmüller, and A. D. MacKerell Jr. 2017. CHARMM36m: an improved force field for folded and intrinsically disordered proteins. *Nature methods*. 14(1):71-73.

50. Phillips, J. C., D. J. Hardy, J. D. C. Maia, J. E. Stone, J. V. Ribeiro, R. C. Bernardi, R. Buch, G. Fiorin, J. Hénin, W. Jiang, R. McGreevy, M. C. R. Melo, B. K. Radak, R. D. Skeel, A. Singharoy, Y. Wang, B. Roux, A. Aksimentiev, Z. Luthey-Schulten, L. V. Kalé, K. Schulten, C. Chipot, and E. Tajkhorshid. 2020. Scalable molecular dynamics on CPU and GPU architectures with NAMD. *J Chem Phys*. 153(4):044130, doi: 10.1063/5.0014475.

51. Rettig, J., F. Wunder, M. Stocker, R. Lichtinghagen, F. Mastiaux, S. Beckh, W. Kues, P. Pedarzani, K. H. Schröter, J. P. Ruppersberg, and et al. 1992. Characterization of a Shaw-related potassium channel family in rat brain. *Embo j*. 11(7):2473-2486, doi: 10.1002/j.1460-2075.1992.tb05312.x.

52. Strang, C., S. J. Cushman, D. DeRubeis, D. Peterson, and P. J. Pfaffinger. 2001. A central role for the T1 domain in voltage-gated potassium channel formation and function. *J Biol Chem*. 276(30):28493-28502, doi: 10.1074/jbc.M010540200.

53. Nanao, M. H., W. Zhou, P. J. Pfaffinger, and S. Choe. 2003. Determining the basis of channel-tetramerization specificity by x-ray crystallography and a sequence-comparison algorithm: Family Values (FamVal). *Proc Natl Acad Sci U S A*. 100(15):8670-8675, doi: 10.1073/pnas.1432840100.

54. Robinson, J. M., and C. Deutsch. 2005. Coupled tertiary folding and oligomerization of the T1 domain of Kv channels. *Neuron*. 45(2):223-232, doi: 10.1016/j.neuron.2004.12.043, http://www.ncbi.nlm.nih.gov/pubmed/15664174 (Research Support, Non-U.S. Gov't Research Support, U.S. Gov't, P.H.S.).

55. Bixby, K. A., M. H. Nanao, N. V. Shen, A. Kreusch, H. Bellamy, P. J. Pfaffinger, and S. Choe. 1999. Zn2+-binding and molecular determinants of tetramerization in voltage-gated K+ channels. *Nature structural biology*. 6(1):38-43, doi: 10.1038/4911.

56. Lu, J., J. M. Robinson, D. Edwards, and C. Deutsch. 2001. T1-T1 interactions occur in ER membranes while nascent Kv peptides are still attached to ribosomes. *Biochemistry*. 40(37):10934-10946, doi: 10.1021/bi010763e.

57. Kosolapov, A., L. Tu, J. Wang, and C. Deutsch. 2004. Structure acquisition of the T1 domain of Kv1.3 during biogenesis. *Neuron*. 44(2):295-307, doi: 10.1016/j.neuron.2004.09.011.

58. Jegla, T. J., C. M. Zmasek, S. Batalov, and S. K. Nayak. 2009. Evolution of the human ion channel set. *Comb Chem High Throughput Screen*. 12(1):2-23, http://www.ncbi.nlm.nih.gov/pubmed/19149488.

59. Liu, P., Q. Ge, B. Chen, L. Salkoff, M. I. Kotlikoff, and Z. W. Wang. 2011. Genetic dissection of ion currents underlying all-or-none action potentials in C. elegans body-wall muscle cells. *J Physiol*. 589(Pt 1):101-117, doi: 10.1113/jphysiol.2010.200683.

60. Weiss, J. L., J. Yang, C. Jie, D. L. Walker, S. Ahmed, Y. Zhu, Y. Huang, K. M. Johansen, and J. Johansen. 1999. Molecular cloning and characterization of LKv1, a novel voltage-gated potassium channel in leech. *Journal of neurobiology*. 38(2):287-299.

61. Schwarz, T. L., B. L. Tempel, D. M. Papazian, Y. N. Jan, and L. Y. Jan. 1988. Multiple potassium-channel components are produced by alternative splicing at the Shaker locus in Drosophila. *Nature*. 331(6152):137-142, doi: 10.1038/331137a0, http://www.ncbi.nlm.nih.gov/pubmed/2448635.

62. Timpe, L. C., Y. N. Jan, and L. Y. Jan. 1988. Four cDNA clones from the Shaker locus of Drosophila induce kinetically distinct A-type potassium currents in Xenopus oocytes. *Neuron*. 1(8):659-667, doi: 0896-6273(88)90165-1 [pii], http://www.ncbi.nlm.nih.gov/pubmed/3272184.

63. Li, X., A. S. Martinson, M. J. Layden, F. H. Diatta, A. P. Sberna, D. K. Simmons, M. Q. Martindale, and T. J. Jegla. 2015. Ether-a-go-go family voltage-gated K+ channels evolved in an ancestral metazoan and functionally diversified in a cnidarian-bilaterian ancestor. *J Exp Biol*. 218(Pt 4):526-536, doi: 10.1242/jeb.110080.

64. Geiger, J. R., and P. Jonas. 2000. Dynamic control of presynaptic Ca(2+) inflow by fast-inactivating K(+) channels in hippocampal mossy fiber boutons. *Neuron*. 28(3):927-939, doi: 10.1016/s0896-6273(00)00164-1.

65. Aldrich, R. W., Jr., P. A. Getting, and S. H. Thompson. 1979. Mechanism of frequency-dependent broadening of molluscan neurone soma spikes. *J Physiol*. 291:531-544, doi: 10.1113/jphysiol.1979.sp012829.

66. Niwa, N., and J. M. Nerbonne. 2010. Molecular determinants of cardiac transient outward potassium current (I(to)) expression and regulation. *J Mol Cell Cardiol*. 48(1):12-25, doi: 10.1016/j.yjmcc.2009.07.013.

67. Pisupati, A., K. J. Mickolajczyk, W. Horton, D. B. van Rossum, A. Anishkin, S. V. Chintapalli, X. Li, J. Chu-Luo, G. Busey, W. O. Hancock, and T. Jegla. 2018. The S6 gate in regulatory Kv6 subunits restricts heteromeric K(+) channel stoichiometry. *J Gen Physiol*. 150(12):1702-1721, doi: 10.1085/jgp.201812121.

68. Post, M. A., G. E. Kirsch, and A. M. Brown. 1996. Kv2.1 and electrically silent Kv6.1 potassium channel subunits combine and express a novel current. *FEBS Lett*. 399(1-2):177-182, doi: S0014-5793(96)01316-6 [pii], http://www.ncbi.nlm.nih.gov/pubmed/8980147.

69. Salinas, M., J. de Weille, E. Guillemare, M. Lazdunski, and J. P. Hugnot. 1997. Modes of regulation of shab K+ channel activity by the Kv8.1 subunit. *J Biol Chem*. 272(13):8774-8780, http://www.ncbi.nlm.nih.gov/pubmed/9079713.

70. Bocksteins, E. 2016. Kv5, Kv6, Kv8, and Kv9 subunits: No simple silent bystanders. *The Journal of general physiology*. 147(2):105-125, doi: 10.1085/jgp.201511507, http://www.ncbi.nlm.nih.gov/pubmed/26755771 (Review).

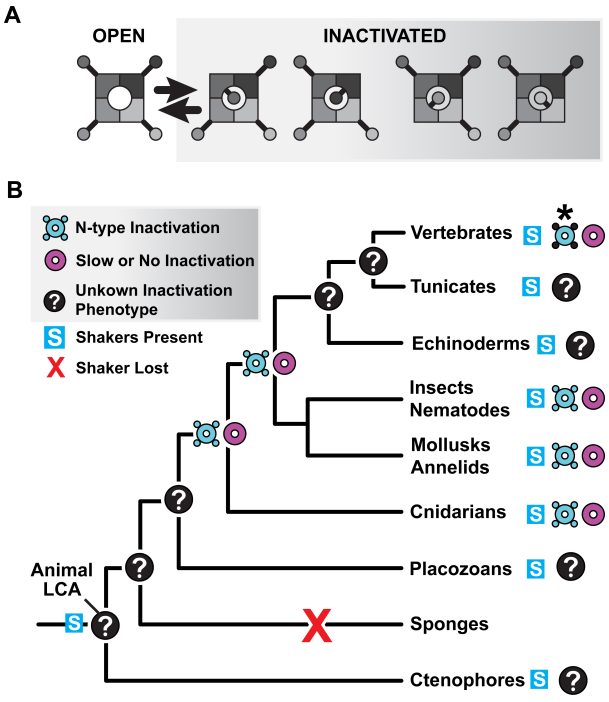

MIShak α-subunits

Shaker subfamily α-subunits with N-type Balls

Other K^+ channel subunits with N-type Balls